ac losses in type-II superconductors in parallel magnetic fields

Antonio Perez-Gonzalez and John R. Clem
Ames Laboratory—U.S. Department of Energy and Department of Physics, Iowa State University, Ames, Iowa 50011
(Received 25 March 1985)

A general critical-state theory, which includes the effects of both flux-line cutting and flux pinning, is used for calculating hysteretic losses in type-II superconductors subjected to an oscillating magnetic field oriented at an arbitrary angle with respect to a bias field, both fields being parallel to the surface. Analytic expressions for the ac losses are obtained for the case that the amplitude of the oscillating field is small compared with the magnitude of the bias field. These expressions reduce to the known ones in two limits: the collinear case, when only flux-pinning losses are present, and the perpendicular case, when only flux-cutting losses are present. A comparison with the experimental results of LeBlanc and Lorrain is made.

I. INTRODUCTION

The hysteretic response of a type-II-superconducting slab subjected to a parallel applied magnetic field that varies in both magnitude and direction is remarkably complex, as has been demonstrated in a series of experiments by Leblanc and co-workers.[1–4] An interesting example of this is the behavior of a superconducting disk rotating relative to a fixed parallel applied magnetic field;[1–3] this corresponds to the case of a stationary superconductor subjected to a parallel applied field that varies in direction but not in magnitude. To explain the resulting behavior has required the development of a general critical-state theory, which includes not only the effects of flux pinning, as in the usual critical-state theory, but also the effects of flux-line cutting.[5–7]

LeBlanc and co-workers also have carried out experiments in which the applied magnetic field varies in both magnitude and direction.[4] They examined two magnetic regimes: the common *collinear* regime, in which an ac field is applied parallel to a dc bias field, and the *noncollinear* regime, in which both an ac field and a dc bias field are applied parallel to a superconducting slab, but with the ac field at an arbitrary angle relative to the dc field. Although the usual critical-state theory can be used to derive expressions for the ac losses in the collinear regime, new equations and new physics must be added to calculate and understand the losses in the noncollinear regime.[5]

In this paper we apply our general critical-state theory[6] to calculate the hysteretic losses of a type-II superconductor in the noncollinear regime. The theory makes use of two fundamental material-dependent quantities: $J_{c\perp}$, the transverse critical current density at the threshold of depinning, and $J_{c\parallel}$, the longitudinal critical current density at the threshold of flux-line cutting. Both $J_{c\perp}$ and $J_{c\parallel}$ depend upon the magnitude of the local magnetic induction B and the absolute temperature T. To obtain analytic expressions for the physical quantities of interest, e.g., electric fields, current densities, and losses per cycle, we assume here that the amplitude of the ac field is sufficiently small that $J_{c\perp}$ and $J_{c\parallel}$ do not change significantly over the cycle. We derive the desired expressions for the ac losses in Sec. II. In Sec. III we apply these expressions to the experiments of Ref. 4, and in Sec. IV we summarize our results and discuss needed extensions of the theory.

II. THEORY

We consider first a semi-infinite, high-κ, irreversible type-II superconductor with surface at $x=0$, to which is applied a dc bias field $\mathbf{B}_0=\hat{\mathbf{z}}B_0$ and an ac field $\mathbf{b}_a(t)$ of amplitude $b_0 \ll B_0$ at an arbitrary angle γ $(0\leqq\gamma\leqq\pi/2)$ with respect to $\mathbf{B}_0$. The net externally applied magnetic induction is $\mathbf{B}_s(t)=\mathbf{B}_0+\mathbf{b}_a(t)$, as sketched in Fig. 1.

It is convenient to write the magnetic induction inside the specimen $(x>0)$ as $\mathbf{B}=B\hat{\boldsymbol{\alpha}}$, where $B=|\mathbf{B}|$ is its

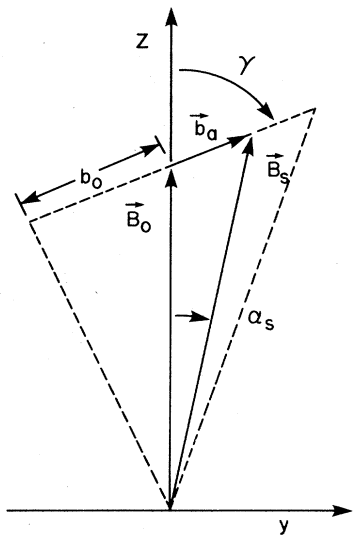

FIG. 1. Sketch of the fields applied parallel to the surface. A dc bias field $\mathbf{B}_0$ is applied in the z direction, and an ac field $\mathbf{b}_a$ is applied parallel to the y-z plane at an angle γ with respect to $\mathbf{B}_0$. To lowest order in b_0, the magnitude $B_s=B_0+b_a\cos\gamma$ of the net applied field oscillates between $B_0\pm b_0\cos\gamma$, and the angle $\alpha_s=b_a\sin\gamma/B_0$ between the net field and the z axis oscillates between $\pm b_0\sin\gamma/B_0$.

magnitude and $\hat{\alpha}$ its direction,

$$\hat{\alpha}=\hat{\mathbf{y}}\sin\alpha+\hat{\mathbf{z}}\cos\alpha \ . \tag{1}$$

We also write the current density $\mathbf{J}$ and the electric field $\mathbf{E}$ in terms of their components parallel and perpendicular to $\mathbf{B}$; i.e., $\mathbf{J}=J_{||}\hat{\alpha}+J_{\perp}\hat{\beta}$ and $\mathbf{E}=E_{||}\hat{\alpha}+E_{\perp}\hat{\beta}$, where $\hat{\beta}=\hat{\alpha}\times\hat{\mathbf{x}}$. We assume that it is a good approximation to take $\mathbf{B}=\mu_0\mathbf{H}$ inside the superconductor, and we ignore any surface-barrier or surface-pinning effects. Using Ampere's law, $\mathbf{J}=\nabla\times\mathbf{H}$ (neglecting the displacement current) and Faraday's law, we obtain

$$J_{||}=\mu_0^{-1}B\frac{\partial\alpha}{\partial x} \ , \tag{2}$$

$$J_{\perp}=-\mu_0^{-1}\frac{\partial B}{\partial x} \ , \tag{3}$$

and

$$\frac{\partial E_{||}}{\partial x}=B\frac{\partial\alpha}{\partial t}+E_{\perp}\frac{\partial\alpha}{\partial x} \ , \tag{4}$$

$$\frac{\partial E_{\perp}}{\partial x}=-\frac{\partial B}{\partial t}-E_{||}\frac{\partial\alpha}{\partial x} \ . \tag{5}$$

The general critical-state model[6,7] states that metastable stationary distributions of B, in which $E_{\perp}=0$, are always such that $J_{\perp}$ obeys

$$|J_{\perp}|\leq J_{c\perp}(B) \ . \tag{6}$$

Similarly, metastable stationary distributions of α, in which $E_{||}=0$, are always such that $J_{||}$ obeys

$$|J_{||}|\leq J_{c||}(B) \ , \tag{7}$$

which can be written, using Eq. (2), as

$$\left|\frac{\partial\alpha}{\partial x}\right|\leq k_{c||}(B) \ , \tag{8}$$

where

$$k_{c||}(B)\equiv\mu_0 J_{c||}(B)/B \ .$$

We assume the material has been through many cycles, so that it possesses a diamagnetic profile near the surface.[7] The magnitude and direction of the external B field are, to first order in b_a (see Fig. 1),

$$B_s=B_0+b_a\cos\gamma \tag{9}$$

and

$$\alpha_s=b_a\sin\gamma/B_0 \ . \tag{10}$$

The B and α profiles are linear in x to lowest order in b_a. Figure 2 shows the extremal B and α profiles,

$$B_{\max}(x)=B_0+b_0\cos\gamma-\mu_0 J_{c\perp}x \ , \tag{11}$$

$$B_{\min}(x)=B_0-b_0\cos\gamma+\mu_0 J_{c\perp}x \ , \tag{12}$$

and

$$\alpha_{\max}(x)=(b_0/B_0)\sin\gamma-k_{c||}x \ , \tag{13}$$

$$\alpha_{\min}(x)=-(b_0/B_0)\sin\gamma+k_{c||}x \ , \tag{14}$$

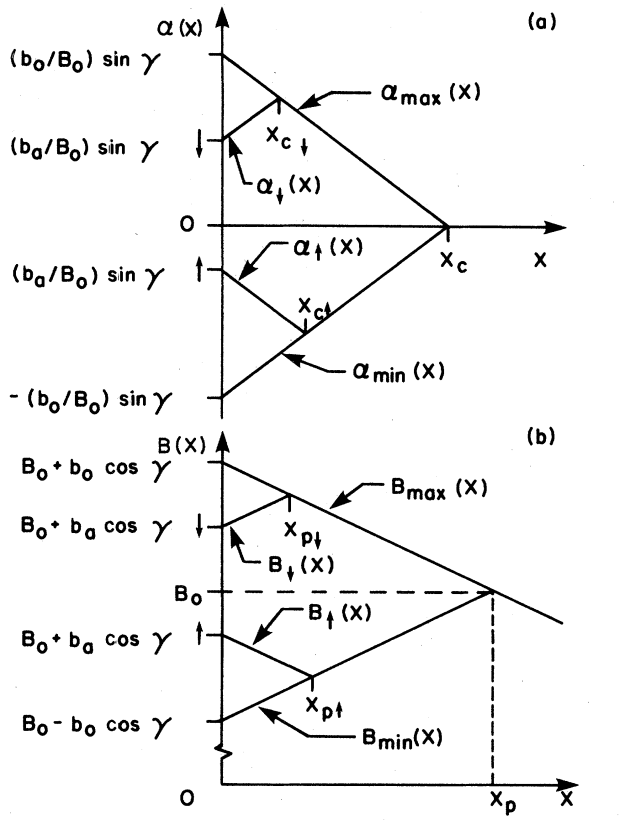

FIG. 2. Sketch of (a) extremal field-angle profiles $\alpha_{\max}$ and $\alpha_{\min}$ and the α_s-increasing and α_s-decreasing profiles $\alpha_{\uparrow}$ and $\alpha_{\downarrow}$, vs x, calculated from $|\partial\alpha/\partial x|=k_{c||}$; (b) extremal field-magnitude profiles $B_{\max}$ and $B_{\min}$ and the B_s-increasing and B_s-decreasing profiles $B_{\uparrow}$ and $B_{\downarrow}$, vs x, calculated from $|\partial B/\partial x|=\mu_0 J_{c\perp}$.

where $J_{c\perp}=J_{c\perp}(B_0)$ and $k_{c||}=k_{c||}(B_0)$. The depths within which B and α change during each cycle are

$$x_p=b_0\cos\gamma/\mu_0 J_{c\perp} \tag{15}$$

and

$$x_c=b_0\sin\gamma/\mu_0 J_{c||} \ , \tag{16}$$

respectively. Note that x_p may be larger than, equal to, or smaller than x_c, depending upon the values of γ, $J_{c\perp}$, and $J_{c||}$. Also shown in Fig. 2 are B and α profiles for the b_a-increasing ($\uparrow$) and b_a-decreasing ($\downarrow$) cases.

The ac loss per unit area per cycle W_a' is given by the time integral over the entire cycle of the Poynting vector,

$$W_a'=\mu_0^{-1}\oint dt\,\hat{\mathbf{x}}\cdot\mathbf{E}(0,t)\times[\mathbf{B}_0+\mathbf{b}_a(t)] \ . \tag{17}$$

Integrating Faraday's law from the surface to a point x_0 sufficiently deep in the superconductor that $\mathbf{E}(x_0,t)=0$, we obtain

$$\hat{\mathbf{x}}\times\mathbf{E}(0,t)=\int_0^{x_0}dx\frac{\partial\mathbf{B}(x,t)}{\partial t} \ . \tag{18}$$

Defining

$$\mathbf{b}(x,t)=\mathbf{B}(x,t)-\mathbf{B}_0 \tag{19}$$

and

$$\Phi'(t)=\int_0^{x_0} dx\, \mathbf{b}(x,t)\ , \tag{20}$$

we obtain

$$W_a'=\mu_0^{-1}\oint dt\, \mathbf{b}_a(t)\cdot\frac{d}{dt}\Phi'(t)\ , \tag{21}$$

where we have made use of the periodicity of $\Phi'(t)$ in time. Denoting values corresponding to the b_a-increasing and b_a-decreasing half-cycles by $\uparrow$ and $\downarrow$, respectively, and defining

$$\Delta\Phi'=(\Phi'_\downarrow-\Phi'_\uparrow)\cdot(\hat{\mathbf{y}}\sin\gamma+\hat{\mathbf{z}}\cos\gamma)\ , \tag{22}$$

we obtain, after integrating by parts and changing variables,

$$W_a'=\mu_0^{-1}\int_{-b_0}^{b_0} db_a\Delta\Phi'\ . \tag{23}$$

Because we desire an expression for W_a' valid to order b_0^3, we need to compute $\Delta\Phi'$ only to order b_0^2. In this approximation Eq. (20) yields

$$\Phi'_\downarrow=\hat{\mathbf{y}}B_0\left[\int_0^{x_{c\downarrow}} dx\,\alpha_\downarrow(x)+\int_{x_{c\downarrow}}^{x_c} dx\,\alpha_{\max}(x)\right]+\hat{\mathbf{z}}\left[\int_0^{x_{p\downarrow}} dx[B_\downarrow(x)-B_0]+\int_{x_{p\downarrow}}^{x_p} dx[B_{\max}(x)-B_0]\right]$$
$$=\left[\hat{\mathbf{y}}\frac{\sin^2\gamma}{4\mu_0 J_{c\|}}+\hat{\mathbf{z}}\frac{\cos^2\gamma}{4\mu_0 J_{c\perp}}\right](b_0^2+2b_0b_a-b_a^2)\ , \tag{24}$$

where we have used

$$x_{c\downarrow}=\frac{b_0-b_a}{2\mu_0 J_{c\|}}\sin\gamma \tag{25}$$

and

$$x_{p\downarrow}=\frac{b_0-b_a}{2\mu_0 J_{c\perp}}\cos\gamma\ . \tag{26}$$

Similarly,

$$\Phi'_\uparrow=\left[\hat{\mathbf{y}}\frac{\sin^2\gamma}{4\mu_0 J_{c\|}}+\hat{\mathbf{z}}\frac{\cos^2\gamma}{4\mu_0 J_{c\perp}}\right](b_a^2+2b_0b_a-b_0^2)\ , \tag{27}$$

such that from Eq. (22)

$$\Delta\Phi'=\left[\frac{\sin^3\gamma}{2\mu_0 J_{c\|}}+\frac{\cos^3\gamma}{2\mu_0 J_{c\perp}}\right](b_0^2-b_a^2)\ . \tag{28}$$

The resulting loss per unit area per cycle from Eq. (23) is

$$W_a'=\frac{2b_0^3}{3\mu_0^2}\left[\frac{\sin^3\gamma}{J_{c\|}}+\frac{\cos^3\gamma}{J_{c\perp}}\right]\ . \tag{29}$$

An alternative derivation using the instantaneous power loss per unit volume, $\mathbf{E}\cdot\mathbf{J}=E_\|J_\|+E_\perp J_\perp$, reveals that the first term on the right-hand side of Eq. (29) arises from flux-line-cutting losses and the second term arises from flux-pinning losses. Thus, W_a' can be expressed as $W_a'=W_{ac}'+W_{ap}'$, where W_{ac}', the flux-line-cutting contribution, depends upon $J_{c\|}$, and W_{ap}', the flux-pinning contribution, depends upon $J_{c\perp}$.

When $\gamma=0$ we have the common ac-loss configuration in which no flux-line cutting occurs and the losses result from flux transport across the array of pinning centers. Equation (29) then reduces to the familiar result[8–10]

$$W_a'=W_{ap}'=\frac{2b_0^3}{3\mu_0^2 J_{c\perp}}\ . \tag{30}$$

When $\gamma=\pi/2$, on the other hand, there is no change in B_s to first order in b_0, and all the losses are associated with flux-line cutting, which changes α but not B during the cycle. Equation (29) then reduces to the result derived in Refs. 5 and 6,

$$W_a'=W_{ac}'=\frac{2b_0^3}{3\mu_0^2 J_{c\|}}\ . \tag{31}$$

The above results give the loss per unit area per cycle for a semi-infinite superconductor or at one surface of a superconducting slab whose thickness is more than twice as large as x_p and x_c [Eqs. (15) and (16)]. We consider next the loss per cycle for a finite slab with surfaces at $x=0$ and $x=X=2x_m$. In this case, the magnitude and direction of the external field are still given by Eqs. (9) and (10), but since two surfaces are now exposed to the changing field, Eq. (17) is the ac loss per unit area per cycle per surface. Equations (15) and (16) are still valid, but now we must allow for the possibility that x_c or x_p can be larger than x_m, the half-thickness of the slab. If $x_c>x_m$ the upper limit x_c in Eq. (24) must be replaced by x_m, and the upper or lower limit $x_{c\downarrow}$ must be replaced by $\min(x_{c\downarrow},x_m)$, the smaller of $x_{c\downarrow}$ and x_m. Similarly, if $x_p>x_m$ the upper limit x_p in Eq. (24) must be replaced by x_m, and $x_{p\downarrow}$ must be replaced by $\min(x_{p\downarrow},x_m)$. These replacements are required by the conditions that (a) $\mathbf{B}$ is symmetric with respect to the midpoint of the slab and (b) $\mathbf{E}(x_m,t)=0$.

To treat the case of a slab of finite thickness, we define two quantities in analogy with Eqs. (15) and (16):

$$b_{0p}=\mu_0 J_{c\perp}x_m/\cos\gamma \tag{32}$$

and

$$b_{0c}=\mu_0 J_{c\|}x_m/\sin\gamma\ . \tag{33}$$

The size of b_0 relative to b_{0p} and b_{0c} determines the degree of penetration of the changing B and α profiles. When $b_0<b_{0p}$ and $x_p<x_m$, the changing B profile penetrates only part way to the slab's midplane; when $b_0>b_{0p}$, full penetration of the changing B profile occurs. Similarly, when $b_0<b_{0c}$ and $x_c<x_m$, the changing α profile penetrates only part way to the slab's midplane; when

$b_0 > b_{0c}$, full penetration of the changing α profile occurs.

The ac loss per cycle per unit area of one surface obtained from Eqs. (23) and (24), is

$$W_a' = \frac{2b_0^3 \sin^3\gamma}{3\mu_0^2 J_{c\parallel}} + \frac{2b_{0p}^2 \cos^3\gamma}{3\mu_0^2 J_{c\perp}}(3b_0 - 2b_{0p}) , \tag{34}$$

when $b_{0p} \leqq b_0 \leqq b_{0c}$,

$$W_a' = \frac{2b_{0c}^2 \sin^3\gamma}{3\mu_0^2 J_{c\parallel}}(3b_0 - 2b_{0c}) + \frac{2b_0^3 \cos^3\gamma}{3\mu_0^2 J_{c\perp}} , \tag{35}$$

when $b_{0c} \leqq b_0 \leqq b_{0p}$, and

$$W_a' = \frac{2b_{0c}^2 \sin^3\gamma}{3\mu_0^2 J_{c\parallel}}(3b_0 - 2b_{0c}) + \frac{2b_{0p}^2 \cos^3\gamma}{3\mu_0^2 J_{c\perp}}(3b_0 - 2b_{0p}) \tag{36}$$

when $b_0 \geqq b_{0c}$ and $b_0 \geqq b_{0p}$.

Equations (29) and (34)—(36) predict the variation of W_a' with γ for fixed b_0 and B_0. When both $x_c < x_m$ and $x_p < x_m$, the γ dependence of W_a' is simple, as seen from Eq. (29); otherwise, the γ dependence of b_{0c} and b_{0p} [Eqs. (32) and (33)] leads to a more complex behavior.

The predicted ac loss per unit volume per cycle is

$$W_v = W_a'/x_m = W_{vc} + W_{vp} ,$$

where W_{vc} and W_{vp} are the flux-line-cutting and flux-pinning contributions, respectively. For fixed γ and b_0 but varying B_0, $J_{c\parallel}(B_0)$, and $J_{c\perp}(B_0)$, it can be shown from the above equations that the maximum value of W_{vc} is

$$W_{vc}^{\max} = \frac{3b_0^2}{4\mu_0} \sin^2\gamma , \tag{37}$$

which occurs at a value of $B_0 = B_{0c}^{\max}$ such that $b_{0c} = 3b_0/4$ or

$$J_{c\parallel}(B_{0c}^{\max}) = 3b_0 \sin\gamma / 4\mu_0 x_m .$$

Similarly, the maximum value of W_{vp} is

$$W_{vp}^{\max} = \frac{3b_0^2}{4\mu_0} \cos^2\gamma , \tag{38}$$

which occurs at a value of $B_0 = B_{0p}^{\max}$ such that $b_{0p} = 3b_0/4$ or

$$J_{c\perp}(B_{0p}^{\max}) = 3b_0 \cos\gamma / 4\mu_0 x_m .$$

Thus, W_v obeys

$$W_v \leqq \frac{3b_0^2}{4\mu_0} , \tag{39}$$

with the equality holding only at a value of B_0 that simultaneously maximizes both W_{vc} and W_{vp}, an unlikely case.

III. COMPARISON WITH EXPERIMENT

The validity of the theoretically predicted γ dependence of W_a' should be checked experimentally using the following procedure. A superconducting slab or disk should be subjected to a parallel dc bias field $\mathbf{B}_0$ and a parallel ac field $\mathbf{b}_a(t)$ of amplitude b_0 ($b_0 \ll B_0$) and angle γ relative to $\mathbf{B}_0$. Measurements of W_a' should be made at $\gamma = 0°$ to determine $J_{c\perp}$ versus B_0 from Eq. (29) or (34); measurements then should be made at $\gamma = 90°$ to determine $J_{c\parallel}$ versus B_0 from Eq. (29) or (35). With $J_{c\perp}(B_0)$ and $J_{c\parallel}(B_0)$ so obtained, Eqs. (29) or (34)—(36) should be used to calculate values of W_a' to be compared with experiment for arbitrary values of b_0, B_0, and γ.

The theory of Sec. II assumes that $J_{c\perp}$ and $J_{c\parallel}$ depend upon the magnitude but not the direction of $\mathbf{B}_0$ relative to the sample. If specimen anisotropy renders this assumption incorrect, the best experimental procedure is to hold the direction of $\mathbf{B}_0$ fixed relative to the specimen while the direction of $\mathbf{b}_a$ is changed. If, on the other hand, the direction of $\mathbf{b}_a$ is held fixed relative to the specimen while the direction of $\mathbf{B}_0$ is changed, the expected angular (γ) dependence of the changeover from flux-line-cutting-dominated to flux-pinning-dominated behavior could well be swamped by the effects of critical-current anisotropy.

Numerous ac-loss measurements have been reported using experimental geometries in which flux-line cutting evidently was involved.[4,11–20] However, because none of these used a procedure like that suggested above, we currently are unable to make a definitive comparison with experiment. Nevertheless, in the following, we attempt to apply the theory of Sec. II to some recent experiments[4] in which flux-line cutting evidently is the dominant loss mechanism. As will be shown, however, there is relatively poor agreement between theory and experiment, presumably because of the complicating influence of critical current anisotropy.

LaBlanc and Lorrain[4] have reported measurements of ac losses in a rectangular specimen of $V_{0.24}Ti_{0.76}$. In their experiments, in the notation of our paper, the amplitude of $\mathbf{b}_a$ was held constant ($b_0 = 0.05$ T) and its direction was fixed relative to the specimen, while $\mathbf{B}_0$ varied in both magnitude and direction. From the authors' $\gamma = 90°$ data [triangular data points in Fig. 1(a) of Ref. 4] we can infer $J_{c\parallel}(B_0)$ vs B_0 as follows. The theoretical loss per unit volume per cycle at $\gamma = 90°$ is

$$W_{vc} = \frac{2b_0^3}{3\mu_0 b_{0c}} \tag{40}$$

for partial penetration of the α profile [Eq. (29)], and

$$W_{vc} = \frac{2b_{0c}}{3\mu_0}(3b_0 - 2b_{0c}) \tag{41}$$

for full penetration of the α profile [Eq. (35)]. Using Eqs. (33), (40), and (41) and the triangular data points of Fig. 1(a) of Ref. 4, combined with the assumption that $J_{c\parallel}(B)$ is a monotonically decreasing function of B, we infer the values of $J_{c\parallel}$ vs B shown as the points in Fig. 3. This behavior of $J_{c\parallel}$ can be approximated over the range $0.5 \leqq B \leqq 2.2$ T by (solid curve, Fig. 3)

$$J_{c\parallel}(B) = (6.9 \times 10^3) B^{-0.633}(1 - B/B_{c2}) \text{ A/cm}^2 , \tag{42}$$

where B is in T and $B_{c2} = 4.0$ T.

The data shown in Fig. 1 of Ref. 4 do not permit us to make a corresponding inference about the values of $J_{c\perp}$

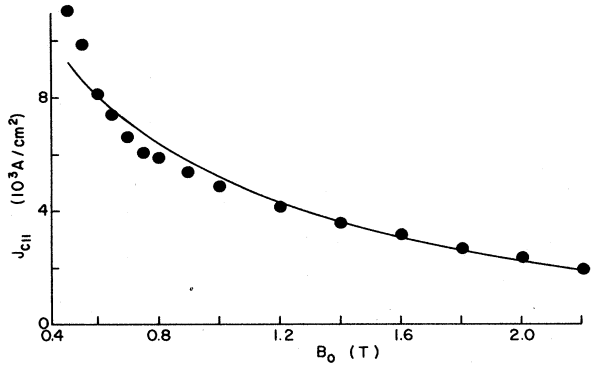

FIG. 3. Experimental values (solid circles) of $J_{c\|}$ vs B_0 from data in Fig. 1(a), Ref. 4, using Eqs. (40) and (41). The solid curve represents Eq. (42).

over the same range. The reported results in the collinear regime ($\gamma=0°$) are restricted to a small range of B_0 for which b_0 and B_0 are comparable in magnitude. We thus assume that

$$J_{c\perp}(B)=J_{c\|}(B)/\chi\ , \tag{43}$$

where χ is a constant independent of B, to calculate the losses when $0°<\gamma<90°$.

Shown in Fig. 4 is a comparison of the calculated losses per unit volume per cycle, obtained from Eqs. (29), (34)—(36), (42), and (43) (solid curves), with the corresponding measured losses given in Fig. 1(a) of Ref. 4 (points). For this comparison the value $\chi=13$ is used, as suggested in Ref. 4. In the experiments the bias field was $B_0=(B_{\|}^2+b_b^2)^{1/2}$, where $b_b=0$ T (triangles) or 0.1 T (squares), the amplitude of the ac field was $b_0=0.05$ T, and the angle γ between the ac field and the net bias field was $\gamma=\tan^{-1}(B_{\|}/b_b)$. For the triangles, $\gamma=90°$, and, for the squares, γ varied from 79° at $B_{\|}=0.5$ T to 87° at $B_{\|}=2.2$ T. The lower solid curve corresponds to the triangular data points ($b_b=0$ T). It fails to fit all the data points only because the empirical equation for $J_{c\|}(B)$ [Eq. (42)] had only two adjustable parameters; using more adjustable parameters would have permitted a better fit. The upper solid curve in Fig. 4 corresponds to $b_b=0.1$ T. The upward shift arises from the increased contribution of flux-pinning losses as γ decreases. The predicted increase in the losses at smaller values of $B_{\|}$, however, is much less than the experimentally observed increase. Since the losses at these values of $B_{\|}$ are still primarily flux-line-cutting losses, we believe that the discrepancy between the theoretical and experimental losses is due to critical current anisotropy, i.e., dependence of $J_{c\|}$ upon the direction of $\mathbf{B}_0$. Although for the triangular data points the direction of $\mathbf{B}_0$ relative to the sample is the same for all $B_{\|}$, the direction of $\mathbf{B}_0$ for the squares differs from the direction for the triangles by an angle $\delta=\tan^{-1}(b_b/B_{\|})$, which varies from 3° at $B_{\|}=2.2$ T to 11° at $B_{\|}=0.5$ T.

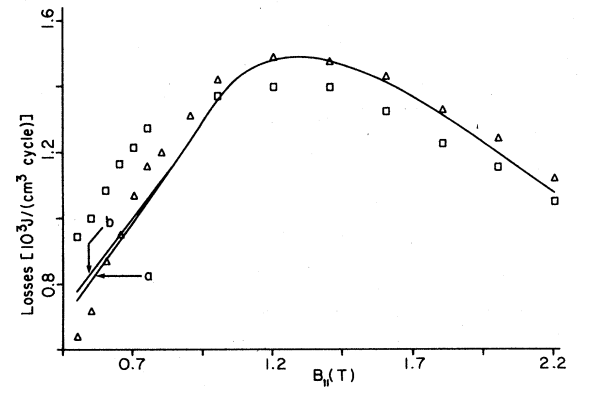

FIG. 4. Experimental (points, Ref. 4) and theoretical (solid curves) values of the losses per unit volume per cycle as calculated from Eqs. (29), (34)—(36), (42), and (43) with $\chi=13$. The ac field was $b_0=0.05$ T and the dc field was $B_0=(B_{\|}^2+b_b^2)^{1/2}$, where (a) $b_b=0$ T (triangles and lower curve) and (b) $b_b=0.1$ T (squares and upper curve).

In the limit of small amplitudes ($b_0\ll B_0$), our general critical-state theory yields profiles that are indistinguishable from those obtained using a double—critical-state model like that of LeBlanc and Lorrain.[4] In agreement with Fig. 4, these authors already noted in Fig. 1(c) of Ref. 4 that their experimental data were not well described by a critical-angle gradient depending only upon the magnitude of $\mathbf{B}$. On the other hand, they obtained good agreement [Fig. 1(d) of Ref. 4] by assuming that the critical-angle gradient depended upon both the magnitude and the direction of $\mathbf{B}$. In the framework of our theory, their approach corresponds to accounting for specimen anisotropy; i.e., they chose an empirical expression that modeled the dependence of $J_{c\|}$ upon both the magnitude of $\mathbf{B}$ and its direction relative to an axis of symmetry in the specimen.

IV. CONCLUSIONS

In Sec. II of this paper we derived explicit expressions for the small-amplitude ac losses occurring when the ac field is at an arbitrary angle γ relative to the dc bias field. When $\gamma\cong 0°$, these losses arise primarily from the transport of vortices across the array of pinning centers, and when $\gamma\cong 90°$ the losses arise primarily from flux-line-cutting processes. We suggested in Sec. III an experimental procedure for a definitive test of the predicted angular dependence. In the absence of experiments well suited for such a test, we applied the theory to the experiments of LeBlanc and Lorrain,[4] in which specimen anisotropy appears to have had an overriding influence.

Several extensions to the theory would be desirable. In deriving the results of Sec. II we assumed that, for a given magnitude of the bias field $\mathbf{B}_0$, the critical current densities were constants, $J_{c\perp}(B_0)$ and $J_{c\|}(B_0)$. This corresponds to the assumption that the B and α profiles during the cycle can be represented by segments of straight lines. This should be a good approximation for small amplitudes ($b_0\ll B_0$). For large ac amplitudes, however, the magnitude of $\mathbf{B}$ inside the sample differs significantly

from B_0 over the cycle, and local values of $J_{c\perp}(B)$ and $J_{c\parallel}(B)$ should be used in computing the time-varying, nonlinear B and α profiles. It therefore would be desirable to extend the theory to permit the calculation of the ac losses for large ac amplitudes in which the B dependence of $J_{c\perp}(B)$ and $J_{c\parallel}(B)$ during the cycle plays an important role. We have developed a numerical method for such a purpose; we plan to present our results in a subsequent publication. It also would be desirable to account for the difference between $\mathbf{B}$ and $\mu_0\mathbf{H}$ inside the superconductor and to include surface barriers against the entry or exit of magnetic flux.

ACKNOWLEDGMENTS

We are grateful to Dr. M. A. R. LeBlanc for stimulating discussions and correspondence. Ames Laboratory is operated for the U.S. Department of Energy by Iowa State University under Contract No. W-7405-Eng-82. This work was supported by The Director for Energy Research, Office of Basic Energy Sciences.

[1]R. Boyer and M. A. R. LeBlanc, Solid State Commun. **24**, 261 (1977).
[2]R. Boyer, G. Fillion, and M. A. R. LeBlanc, J. Appl. Phys. **51**, 1692 (1980).
[3]J. R. Cave and M. A. R. LeBlanc, J. Appl. Phys. **53**, 1631 (1982).
[4]M. A. R. LeBlanc and J. P. Lorrain, J. Appl. Phys. **55**, 4035 (1984).
[5]J. R. Clem, Phys. Rev. B **26**, 2463 (1982).
[6]J. R. Clem and A. Perez-Gonzalez, Phys. Rev. B **30**, 5041 (1984).
[7]A. Perez-Gonzalez and J. R. Clem, Phys. Rev. B **31**, 7048 (1985).
[8]H. London, Phys. Lett. **6**, 162 (1963).
[9]C. P. Bean, Rev. Mod. Phys. **36**, 31 (1964).
[10]J. R. Clem, J. Appl. Phys. **50**, 3518 (1979).
[11]R. Gauthier, Ph.D. thesis, University of Ottawa, 1976.
[12]R. Gauthier and M. A. R. LeBlanc, IEEE Trans. Magn. **MAG-13**, 560 (1977).
[13]A. Lachaine, Ph.D. thesis, University of Ottawa, 1976.
[14]A. Lachaine, M. A. R. LeBlanc, and J. P. Lorrain, Physica (Utrecht) **107B**, 433 (1981).
[15]A. Lachaine and M. A. R. LeBlanc, IEEE Trans. Magn. **MAG-11**, 336 (1975).
[16]Y. Nakayama, in *Proceedings of the 4th International Cryogenic Engineering Conference,* edited by K. Mendelssohn (IPC Science and Technology Press, Guildford, 1972), p. 133.
[17]Y. Yakayama, Y. Koike, and T. Toyoda, in *Proceedings of the 5th International Cryogenic Engineering Conference,* edited by K. Mendelssohn (IPC Science and Technology Press, Guildford, 1974), p. 129.
[18]M. Sugahara and S. Kato, Appl. Phys. Lett. **19**, 111 (1971).
[19]M. Sugahara and N. Yamada, Jpn. J. Appl. Phys. **9**, 1531 (1970).
[20]H. F. Taylor, Appl. Phys. Lett. **11**, 169 (1967).